THE OBSERVATION AND STUDY OF ELP V5-120 CONFORMATIONAL CHANGES

A Thesis

by

QIAN ZHOU

Submitted to the Office of Graduate Studies of
Texas A&M University
in partial fulfillment of the requirements for the degree of

MASTER OF SCIENCE

Approved by:

Chair of Committee,	Paul Cremer
Committee Members,	Kevin Burgess
	Jaime Grunlan
Head of Department,	David Russell

December 2012

Major Subject: Chemistry

ABSTRACT

Elastin-like polypeptides (ELPs) consist of simple pentapeptide repeats which can be easily modified by substituting various amino acid residues to control its properties. This provides an ideal platform for studying hydrophobic collapse and secondary/tertiary structure formation. In this thesis, the collapse process of ELP was studied with differential scanning calorimetry (DSC). In DSC thermal cycling, a clear conformational transition was observed. Also, a transiently stable state of ELP V_5-120 was noted and it was found that the formation of this state was related to temperature, ramping rate and stabilization time. To explain this, a conformational redistribution model is proposed in which there are two conformations in the ELP solution below its transition temperature. However, after the system is heated up and cooled back down, one of the conformations remains the same while the other one changes to two new conformations. After the conformational distribution is done, the ELP stays in a transiently stable state before gradually shifting back to the original, pre-heat-treatment state. Bi-Gaussian fitting was used to fit DSC response curve and monitor the changes of the different conformations in the system. The influence of ramping rate on the process of conformational redistribution was explained through the equilibration time at each temperature point through heating and cooling. Overall, the ELP V_5-120 system is in a dynamic conformational equilibrium, and the equilibration time is much longer than earlier expectations.

TABLE OF CONTENTS

LIST OF FIGURES

Page

LIST OF TABLES

Page

CHAPTER I

INTRODUCTION

Objective

Over many decades, numerous studies have been carried out on the folding of proteins to their native functional states: investigating folding mechanisms[1-4], energetics[5,6], and intermediates[2,7,8]. Currently, energy landscapes are used to describe how unfolded polypeptides search down funnel-like energy profiles towards their native structures[7]. Each polypeptide has a specific energy funnel and local minima, where the polypeptide may get trapped and form partially folded structures, which can lead to misfolding or aggregation. Some typical methods used to probe the folding mechanism involve utilizing mutants of native proteins[9,10], focusing on denatured states[11-13], studying osmolyte effects[14-16], and using simple model peptides[17,18]. Elastin-like polypeptides (ELPs) are a type of model peptides commonly used to study protein folding behavior. They are believed to undergo reversible transitions during heating and cooling[19]. In this thesis, differential scanning calorimetry is used to study the thermal transition of ELP V_5-120 and elucidate the collapse mechanism.

Elastin-like Polypeptides

Elastin-like polypeptides (ELPs) are a class of polypeptides that are inspired by the amino acid sequence of the natural protein elastin. They are composed of the repeating pentapeptide sequence Valine-Proline-Glycine-X-Glycine (VPGXG, where X is any amino acid except Proline)[20]. ELPs are highly soluble in water, but they become a

turbid colloidal suspension upon heating. The transition temperature of this process is usually referred to as lower critical solution temperature (LCST)[21]. The LCST for a given ELP is highly reproducible and is shown to be dependent on a number of factors such as concentration[22], addition of cosolutes or salts to the solution[21,23,24], pH and temperature[25]. Most experiments in this thesis were conducted using ELP V_5-120, which has 120 repeat units of VPGVG with a total molecular weight around 50,000 Daltons. The LCST of the V5-120 was measured with an Optimelt MPA100 (Stanford Research Systems, Sunnyvale, CA) at a concentration of 6.4 mg/mL at a ramp rate of 0.5 °C/min. The LCST was found to be 29.18 ± 0.01 °C.

ELP Conformations and Detection Methods

Although the collapsed ELPs' structure remains unclear, it is believed to contain type II β-turn, β-spiral or β-sheet structures[26-28]. The Cremer group has performed circular dichroism (CD) and ATR/FTIR measurements to investigate the ELPs' structures. In CD spectra, ELPs with hydrophobic or polar side chains all show a negative peak at 225 nm and a small positive peak around 212 nm, which indicate type II *β*-turn structure. There is also a negative peak at 198 nm resulting from random coil structure[29]. In the amide I region (around 1600 cm^{-1} to 1700 cm^{-1}), FTIR spectroscopy of ELPs shows a peak with shoulders that can be assigned to three peaks near 1619, 1663 and 1644 cm^{-1}. The first two peaks are considered to come from *β*-turn and *β*-aggregation, and the last, central peak arises from random coil structure[29]. In a solid-state NMR study of $(VPGVG)_3$, the measurements of C—H and C—N distance between

the two Valine residues of the central pentapeptide and also its torsion angles indicate a coexistence of two conformations in this short ELP: 35% type II β-turn and 65% distorted β-strand.[28] It is believed that the conformational shift between these two structures explains the mechanism of elasticity, and that water plays an important role in facilitating the breaking and formation of hydrogen bonds during the equilibration[28]. In this thesis, DSC was used to monitor the conformational shifts of ELP V_5-120 and see how ramping rate and waiting time affect the process. CD measurements were also applied to confirm the secondary structures of polypeptides. Through these measurements, it was found that ELP conformations are concentration dependent.

CHAPTER II

OBSERVATION OF ELP CONFORMATIONAL CHANGES

Introduction

ELPs are known to collapse and form a cloudy solution upon heating[30,31]. If the collapsed ELPs contain secondary structures like type II β-turn, β spiral or distorted β-sheet as mentioned earlier, and the ELPs in solution below LCST are mostly random coils, this conformational transition should be observable by DSC. Studies show that ELP conformations will revert without much hysteresis upon fast heating[27], however, aqueous two phase system formation may hinder this process if the solution temperature is cycled slowly enough. In this thesis, 0.5 degree per minutes (dpm) and 0.15 dpm ramping rates are used for DSC thermal scans to observe how heat capacity changes with temperature. Circular dichroism was also used to observe the structure of ELP V_5-120 at various concentrations.

Experimental Procedures

The ELP V_5-120 used herein was expressed in BLR(DE3) *E. coli* competent cells according to standard procedures[21,29]. All plasmids were obtained from the Chilkoti Group at Duke University. The plasmids with the desired DNA sequence were incubated on ice with *E. coli* cells for two minutes, and then transferred for electroporation. Immediately after electroporation, autoclaved TB media with ampicillin was added and the whole solution was incubated for an hour at 37 °C in a shaker. The incubated cells were then spread on agar plates to form a thin layer and left at 37 °C for 12 – 15 hours

with gentle shaking to grow cultures. A single culture was picked and rinsed with media before transferring to the culture flask and incubating at 37 °C overnight. The brown solution obtained through DNA expression was the stock culture and was used for ELP expression.

To express ELP, the stock solution was centrifuged first to separate cells from the stock media. The cells were then dissolved into fresh autoclaved media and allowed to grow for 24 hours. The solution was centrifuged and the cells were dissolved in cold phosphate buffer solution (PBS). This solution was sonicated to lyse the cells and centrifuged twice. Polyethylemine was added to the solution to remove insoluble DNA and RNA. 2 M sodium chloride was then added to the supernatant and the mixture was incubated at 50 °C for one hour until it turned cloudy. The solution was centrifuged again and the collected pellets were stored on ice. The pellets were then dissolved in cold PBS and underwent thermal cycling at 4 °C and 90 °C three times for further purification. The absorbance of the resulting solution was measured at 280 nm by UV/Vis to verify the concentration. The extinction coefficient of ELP is 5690 M^{-1} cm^{-1}. The solution was then dialyzed in 18 MΩ water for 3 days and stored at 4 °C.

DSC measurements were run with a VP-DSC MicroCalorimeter (MicroCal, LLC, Northampton, MA). All samples were degassed with a ThermoVac (MicroCal, LLC, Northampton, MA) for 10 minutes at 15 °C. ELP concentration was 6.4 mg/mL (0.128 mM) unless other specified. The sample volume was 500 μL. Before each measurement, the sample and control cell were held at 15 °C for an hour to equilibrate the temperature. The scan range is from 15 °C to 45 °C. A wider range (4 °C to 60 °C)

was also studied and showed results very similar to the shorter range ones. Thus, the shorter range measurements are exclusively addressed herein. Thermal scans consisted of an upward ramping from 15 °C to 45 °C first and then a downward ramping from 45 °C to 15 °C without a waiting period between the two halves of the cycle. Most measurements were done for more than ten cycles continuously to observe ELP's thermal behavior. All the DSC figures enclosed show the upward temperature sweep and are labeled by the number of the cycle. For example, No. 11 means the upward temperature sweep of the 11^{th} scan after ten completed full cycles. When studying the stability of ELP V_5-120's transient states, 13 scans for each sample were run varying the waiting time preceding the 13^{th} upward sweep for each measurement. The deviation of eight parallel scans was 0.2 °C for the peak position and 3.9 kcal mol^{-1} $°C^{-1}$ for peak height.

The CD measurements were performed with an AVIV model 202SF circular dichroism spectrometer (Aviv Instruments, Lakewood, NJ). Spectra were measured in 1 nm steps from 180 to 250 nm with 20 s averaging times. Samples were put in a cuvette with a 1 cm path length at concentrations of 0.032, 0.1 and 0.32 mg/mL. Higher concentrations caused significant interference in spectra due to the opacity of the collapsed ELP, therefore, the samples were only run under 25 °C.

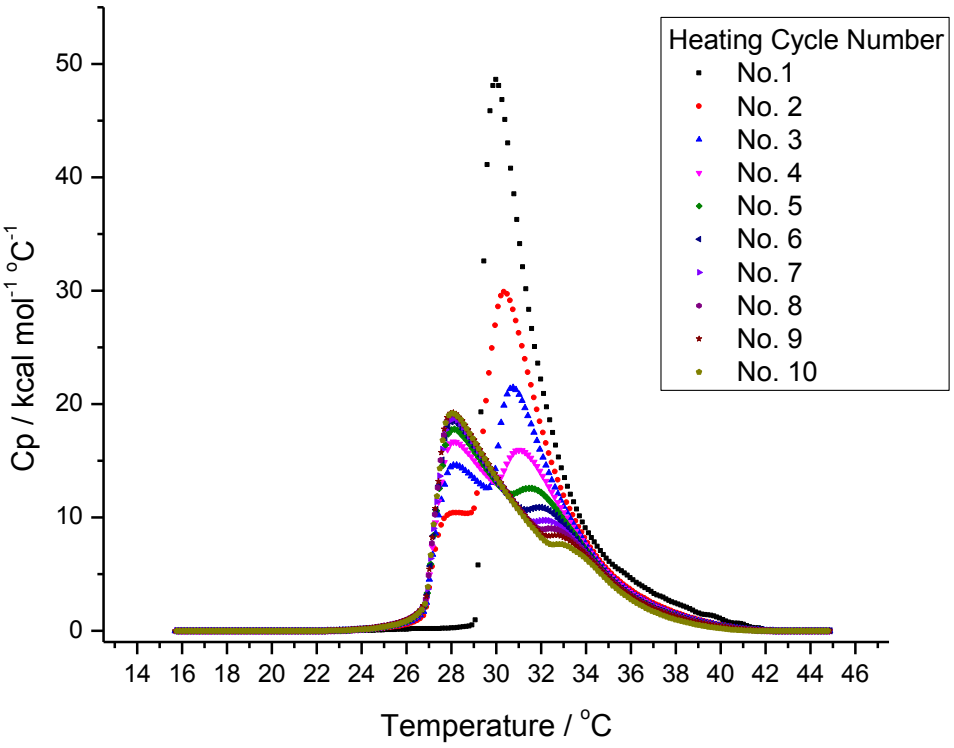

Figure 1. DSC thermal cycling with ELP V_5-120 in water

Results and Discussion

Figure 1 above shows the heat capacity change during the upward temperature sweeps of the first 10 thermal cycles in the system of ELP V_5-120 in pure water with the ramp rate of 0.5 dpm.

It is clearly seen from the DSC plots that there are two transitions during the heating of aqueous ELP V_5-120 solution. The peak around 30°C decreases and shifts right to about 33 °C while a new peak rises up around 28°C. It is believed that this new peak results from a transiently stable ELP state that consisted of a new conformational distribution and that this new peak dominates after approximately 10 thermal cycles.

If there was a conformational shift when the sample was heated up, it would shift back after cooling. To test if the new peak appearing from the second cycle onward was a result of insufficient equilibration time, the latent time between the first and second cycles was varied. After the sample was cooled down to 15 °C at the end of the first cycle, the system was held for 0, 6, 12, 48 and 84 hours and then run for the second thermal cycle. The results are shown below in Figure 2.

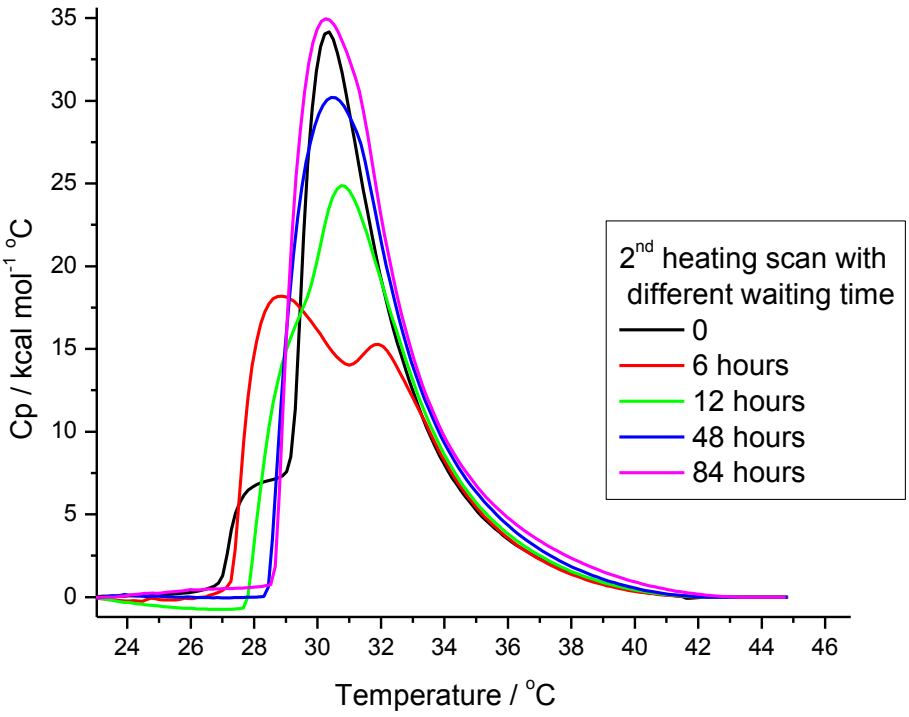

Figure 2. Second up-scans of ELP V_5-120 in water with various waiting times

It is clearly seen that as the waiting time was increased, the new peak diminished and the original peak reverted to its original height and position. Therefore, these conformational changes are reversible. To better estimate the stability of the transiently stable state, the thermal cycle was run 12 times, until the new peak dominated the graph. The 13th cycle was then run after 24 (black), 48 (red) and 120 (blue) hours. Results are shown below in Figure 3:

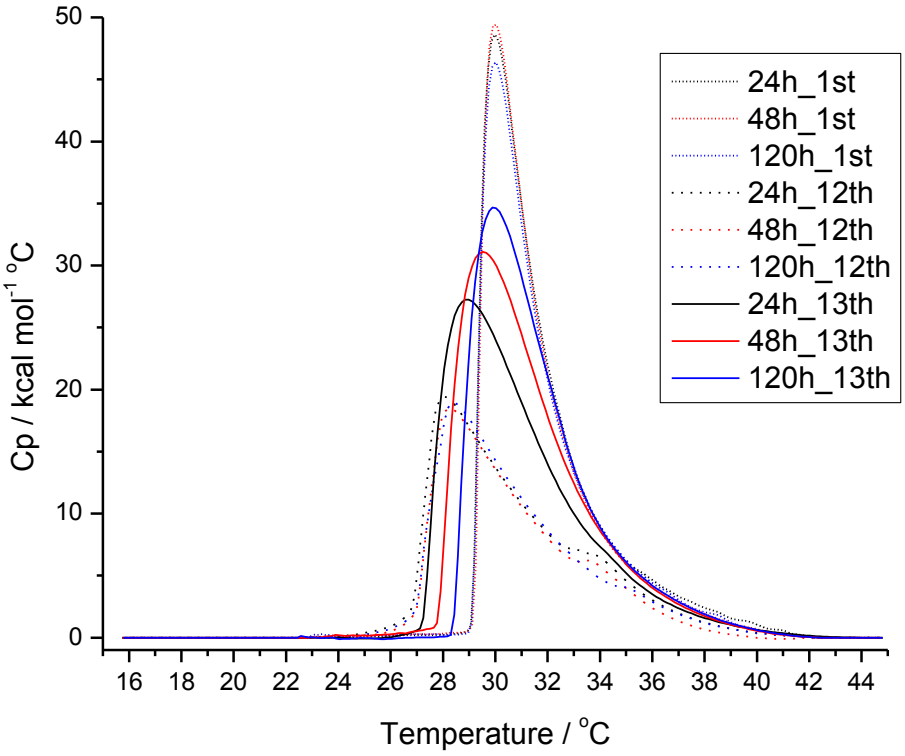

Figure 3. ELP V_5-120 thermal scans with various waiting time before the 13th scan

It can be seen from the graph that as the waiting time increased; the peak shifted to higher temperatures and looked more similar to the original scans. It is reasonable to assume that after waiting for an even longer time, the ELP would move back to the original state before thermal cycling.

The ramping rate was also varied to see how time dependent this transition was. Thermal cycles were run with the same ELP at 0.15 dpm and compared to the results run at 0.5 dpm. It turned out the second thermal scan in the slow ramping rate behaved very

similarly to the ninth thermal scan of the fast ramping rate. The two curves were shown in Figure 4.

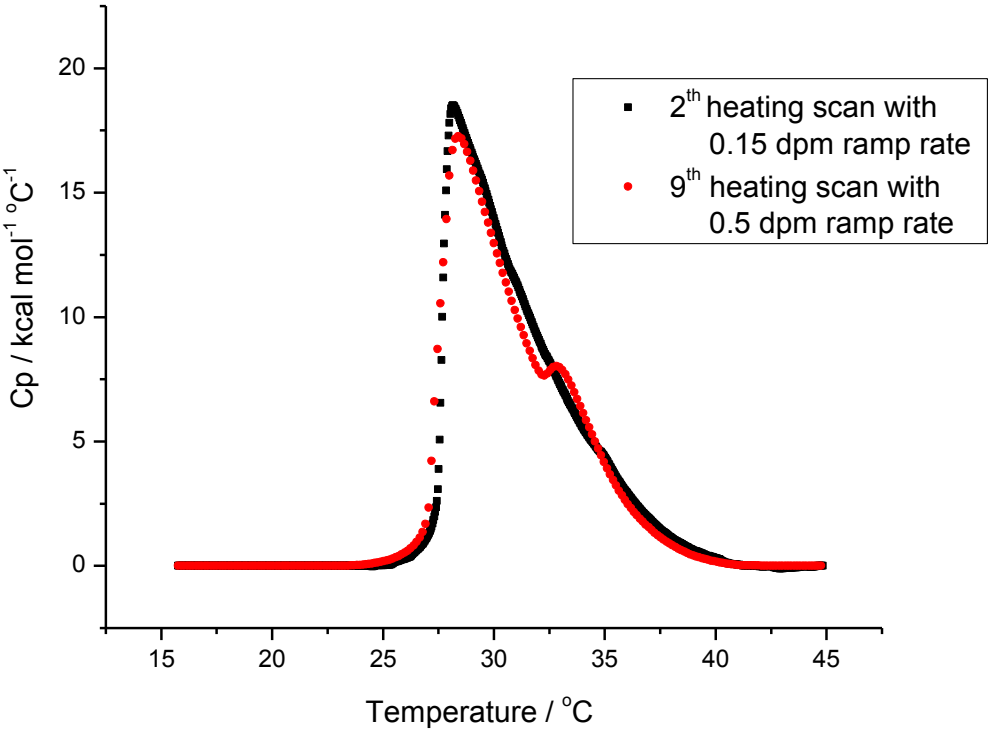

Figure 4. Comparison of heating scan at two different ramp rates.

CHAPTER III

STUDY OF ELP CONFORMATIONAL CHANGES

Introduction

Before we analyze the relation of the thermal scan curve and ELP states transition, it is important to deconvolute the peaks first. Bi-Gaussian fitting was used for the curves since the peaks showed two distinct peak widths for left and right sides. Also bi-Gaussian fitting is widely used in various fields, such as gas chromatography[32], mutational protein stability distribution[33] and proton transfer in membrane proteins[34]. The fitting equation is shown in the equation below[35].

$$y = y_0 + He^{-0.5\left(\frac{x-x_c}{w_1}\right)^2} \quad (x < x_c)$$

$$y = y_0 + He^{-0.5\left(\frac{x-x_c}{w_2}\right)^2} \quad (x \geq x_c)$$

In this equation, y_0 is the baseline, H is the peak height, x_c is the peak position, w_1 and w_2 are the widths of the left and right side of the fitting peak. This equation was used to fit the first ten thermal scans and it emerged that the first scan could be fit into two peaks and the rest of the scans could be fit into three peaks. Peak position and height are listed in Table 1 and the fitting graphs are in the appendix.

Table 1. Parameters of the fitting of DSC thermal scans

Heating Cycle #	**Area 1 %**	**Peak 1 Position °C**	**Area 2 %**	**Peak 2 Position °C**	**Area 3 %**	**Peak 3 Position °C**
1st	N/A	N/A	78.5	29.7	21.5	34.5
2nd	23.5	27.8	61.4	30.3	15.0	34.5
3rd	46.8	28.0	39.0	30.7	14.1	34.5
4th	50.6	28.0	34.6	31.4	14.9	34.6
5th	58.3	28.0	26.5	32.0	15.2	34.8
6th	64.9	27.9	21.7	32.5	13.4	34.9
7th	63.3	27.9	19.0	32.7	17.7	34.5
8th	65.5	27.9	17.5	32.7	17.0	34.3
9th	67.2	27.9	17.5	32.7	15.2	34.5
10th	71.2	27.9	15.9	32.9	12.9	34.6

In the table, Peak 1, 2 and 3 refer to the peaks from left to right in the graph. Area % is the percentage of the area between the peak and baseline in the whole fitting range, and peak position is the temperature where the peak's maximum value is. It can be seen that, the first and third peaks remain in the same position while the second one moves to higher temperatures. For the area percentages, the first peak rises up and the second peak sinks down. The percentage of the third peak remains around 15.7%.

Hypothesized Theory

According to the peak analyses, there should be two states of ELP before the thermal sweep and three states after it undergoes thermal cycling. Each thermal treatment shifts the ELP to the new state a little more until it dominates the ELP's conformation in the solution. It is believed that random coil/strand and β-turn/aggregation structures exist in the system as discussed earlier[28,29] which may correspond to the two states in the beginning. The new state shows up from the second scan onward and is believed to be self-aggregated ELP molecules. The Peak 2 data show that the loose strand or coil structure decreases with each subsequent thermal cycle. The position of Peak 2 also shifts to the right, which indicates there may be structure rearrangement during the process. The position and area percentage of Peak 3 remains about the same, so this tight turn/aggregation structure is very stable and does not change through heat treatment. Overall, the ELP strands intertwine together and form visible aggregation above the LCST; when they cool down, the intermolecular forces decrease and the ELP molecules separate, thus the solution turns clear again; however, individual ELP molecules may still be self-aggregated and need a long time to revert to lower energy conformations. Because the thermal cycles are run continuously, those molecules remain in the transient conformations during the next thermal cycle, and the appearance and dominance of Peak 1 are observed. At the end of the continuous thermal cycles, the majority of ELP has adopted the self-aggregated conformation and the whole system is in the transient state. The whole experiment proves that ELP collapse is a reversible

process; however, this process is more complicated and takes place more slowly than previously thought.

Results and Discussion

To better discuss the results, the positions and areas of the peaks are shown below in Figures 5 and 6.

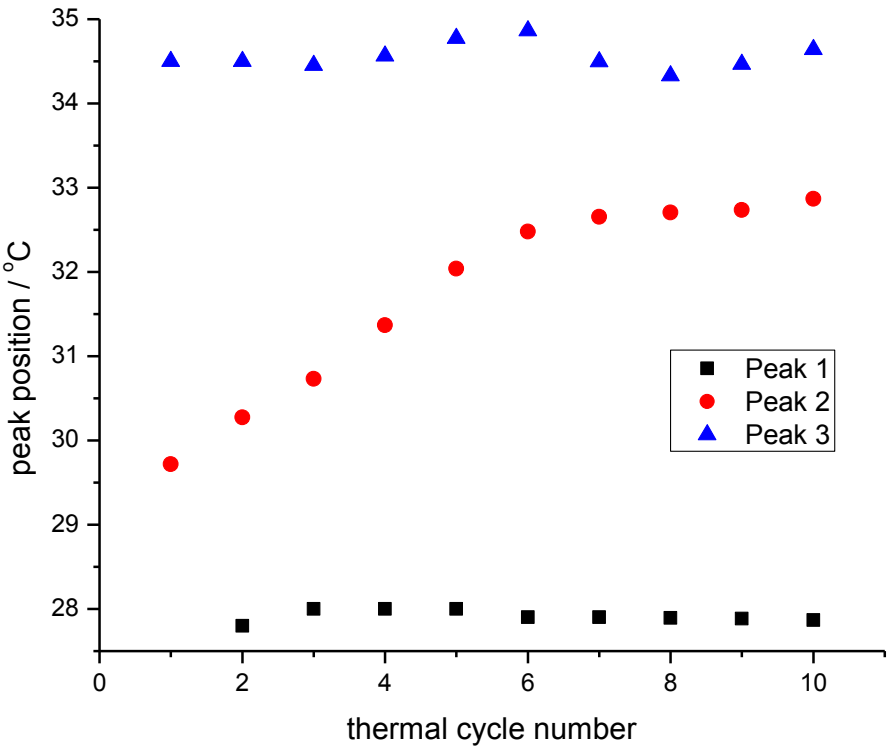

Figure 5. Changes of peak positions of ELP V_5-120 during thermal cycling

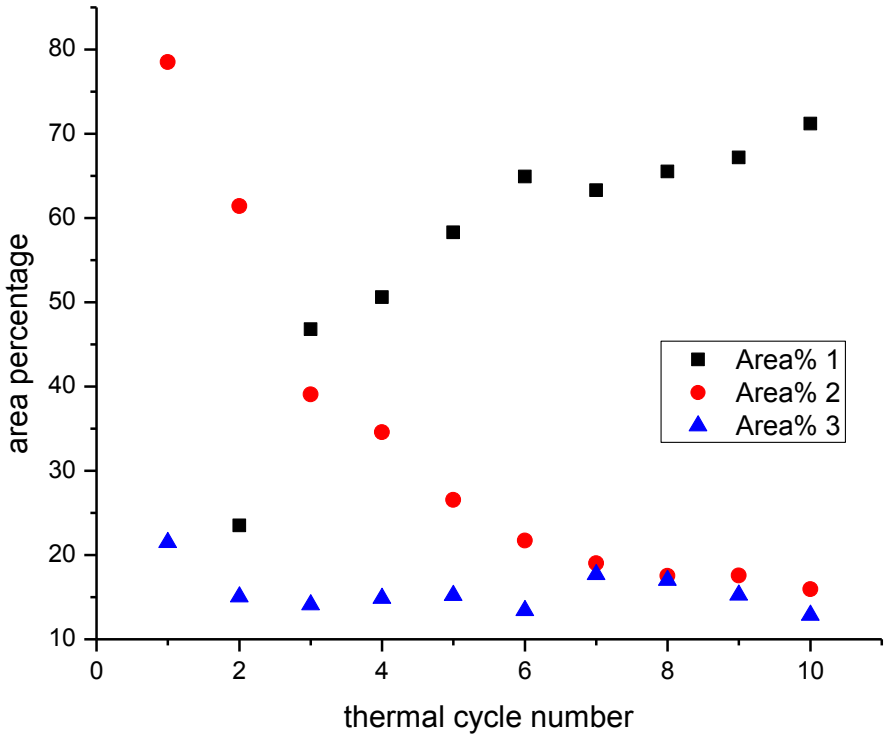

Figure 6. Changes of areas of ELP V_5-120 during thermal cycling

It is clearly seen from the graphs that Peak 1's position remains the same while the area percentage increases, which indicates the accumulation of a new self-aggregated state; Peak 2's position moves to a higher temperature but the area percentage decreases, which suggests that the loose coil structure has changed to a tighter or more tangled structure, and a portion of it has changed conformation entirely and contributes to the structure of Peak 1; Peak 3's position and area percentage both remain the same during heat treatment, it is believed that the tight structure here is thermally stable and does not

change during collapse. These results match well with the theory that the ELP system has coexisting conformations and those conformations are redistributed and finally form the transiently stable state after thermal treatment.

Figures 2 and 3 demonstrate that these conformationally redistributed processes are reversible either in the middle or near the end of the processes. Figure 2 shows that if the ELP system is left to sit after one thermal cycle, it gradually changes back to the original state before thermal cycling. Compared to the trials without a waiting period, the second heating scan after waiting 6 hours shows a shift to higher temperature for both peaks. For longer waiting times, the shoulder peak shifts from left to right as can be seen in the 12, 48 and 84 hours trials. Although in the 84 hour trial the second heating scan did not completely revert to the original position, it is reasonable to assume that if the waiting time is long enough, it will eventually return to the same state as before the first cycle. This demonstrates that the conformational change in ELP collapse upon heating is time dependent and the equilibration time is much longer than expected.

Figure 3 shows that after the transiently stable state dominates the ELP conformation, the redistribution process will still cause the ELP to revert back to the original state. It can be seen that as the waiting time is increased from 24 hours to 120 hours, the peak shifts right and the height rises. The peak also becomes narrower and looks more similar to the original scan. This result also shows that the reverse process slows asymptotically as it approaches the original state. An estimation is that the time for total recovery would be approximately one month.

The different ramping rates also show that the conformational redistribution process is temperature and time related. In the 0.15 dpm scan, at each temperature point, the ELP is held above the LCST long enough to form the hypothesized self-aggregated structure, however, when it is cooled down, the time is not long enough to untangle those aggregations, so it takes fewer thermal cycles to achieve the same transiently stable state. As shown in figure 4, the second thermal scan of 0.15 dpm rate showes a result similar to the ninth thermal scan at the 0.5 dpm rate.

CHAPTER IV

CONCLUSION

In summary, the ELP V_5-120 system was studied by DSC and it was found that different conformations coexist in the system and they are redistributed during thermal treatment. This process is reversible, and temperature and time dependent. The reversibility shows up both in the middle and end of the process. The ELP stays in a transiently stable state after continuous heating and cooling cycles. In this state, the ELP conformational distribution was different from the original ELP solution stored below LCST. It also showed that ELP collapse and its reverse process take place on a much longer time scale than earlier studies have indicated.

REFERENCES

(1) Frousios, K.; Iconomidou, V.; Karletidi, C.-M.; Hamodrakas, S. *BMC Structural Biology* **2009**, *9*, 44.

(2) Hart, T.; Hosszu, L. L. P.; Trevitt, C. R.; Jackson, G. S.; Waltho, J. P.; Collinge, J.; Clarke, A. R. *Proceedings of the National Academy of Sciences* **2009**, *106*, 5651-5656.

(3) Schneider, C. P.; Trout, B. L. *The Journal of Physical Chemistry B* **2009**, *113*, 2050-2058.

(4) Street, T. O.; Bolen, D. W.; Rose, G. D. *Proceedings of the National Academy of Sciences* **2006**, *103*, 13997-14002.

(5) Baldwin, R. L. *Journal of Molecular Biology* **2007**, *371*, 283-301.

(6) Auton, M.; Bolen, D. W. *Proceedings of the National Academy of Sciences of the United States of America* **2005**, *102*, 15065-15068.

(7) Jahn, T. R.; Radford, S. E. *FEBS Journal* **2005**, *272*, 5962-5970.

(8) Hédoux, A.; Guinet, Y.; Paccou, L. *The Journal of Physical Chemistry B* **2011**, *115*, 6740-6748.

(9) Morii, H.; Uedaira, H.; Ogata, K.; Ishii, S.; Sarai, A. *Journal of Molecular Biology* **1999**, *292*, 909-920.

(10) Fu, H.; Grimsley, G. R.; Razvi, A.; Scholtz, J. M.; Pace, C. N. *Proteins: Structure, Function, and Bioinformatics* **2009**, *77*, 491-498.

(11) Fu, H.; Grimsley, G.; Scholtz, J. M.; Pace, C. N. *Protein Science* **2010**, *19*, 1044-1052.

(12) Bennion, B. J.; Daggett, V. *Proceedings of the National Academy of Sciences of the United States of America* **2003**, *100*, 5142-5147.

(13) Lee, M.-E.; van der Vegt, N. F. A. *Journal of the American Chemical Society* **2006**, *128*, 4948-4949.

(14) Arakawa, T.; Timasheff, S. N. *Biophysical Journal* **1985**, *47*, 411-414.

(15) Auton, M.; Ferreon, A. C. M.; Bolen, D. W. *Journal of Molecular Biology* **2006**, *361*, 983-992.

(16) Mukaiyama, A.; Koga, Y.; Takano, K.; Kanaya, S. *Proteins: Structure, Function, and Bioinformatics* **2008**, *71*, 110-118.

(17) Bolen, D. W. *Biochemistry* **2004**, *43*, 1329-1342.

(18) Scholtz, J. M.; Barrick, D.; York, E. J.; Stewart, J. M.; Baldwin, R. L. *Proceedings of the National Academy of Sciences* **1995**, *92*, 185-189.

(19) Reguera, J.; Lagarón, J. M.; Alonso, M.; Reboto, V.; Calvo, B.; Rodríguez-Cabello, J. C. *Macromolecules* **2003**, *36*, 8470-8476.

(20) Meyer, D. E.; Chilkoti, A. *Biomacromolecules* **2004**, *5*, 846-851.

(21) Cho, Y.; Zhang, Y.; Christensen, T.; Sagle, L. B.; Chilkoti, A.; Cremer, P. S. *The Journal of Physical Chemistry B* **2008**, *112*, 13765-13771.

(22) Zhang, Y.; Trabbic-Carlson, K.; Albertorio, F.; Chilkoti, A.; Cremer, P. S. *Biomacromolecules* **2006**, *7*, 2192-2199.

(23) Reguera, J.; Urry, D. W.; Parker, T. M.; McPherson, D. T.; Rodríguez-Cabello, J. C. *Biomacromolecules* **2007**, *8*, 354-358.

(24) Chen, X.; Flores, S. C.; Lim, S.-M.; Zhang, Y.; Yang, T.; Kherb, J.; Cremer, P. S. *Langmuir* **2010**, *26*, 16447-16454.

(25) Nicolini, C.; Ravindra, R.; Ludolph, B.; Winter, R. *Biophysical Journal* **2004**, *86*, 1385-1392.

(26) Serrano, V.; Liu, W.; Franzen, S. *Biophysical Journal* **2007**, *93*, 2429-2435.

(27) Schmidt, P.; Dybal, J.; Rodriguez-Cabello, J. C.; Reboto, V. *Biomacromolecules* **2005**, *6*, 697-706.

(28) Yao, X. L.; Hong, M. *Journal of the American Chemical Society* **2004**, *126*, 4199-4210.

(29) Cho, Y.; Sagle, L. B.; Iimura, S.; Zhang, Y.; Kherb, J.; Chilkoti, A.; Scholtz, J. M.; Cremer, P. S. *Journal of the American Chemical Society* **2009**, *131*, 15188-15193.

(30) Maeda, I.; Fukumoto, Y.; Nose, T.; Shimohigashi, Y.; Nezu, T.; Terada, Y.; Kodama, H.; Kaibara, K.; Okamoto, K. *Journal of Peptide Science* **2011**, *17*, 735-743.

(31) Cirulis, J. T.; Keeley, F. W. *Biochemistry* **2010**, *49*, 5726-5733.

(32) Le Vent, S. *Analytica Chimica Acta* **1995**, *312*, 263-270.

(33) Le Botlan, D.; Helie-Fourel, I. *Analytica Chimica Acta* **1995**, *311*, 217-223.

(34) Narayan, S.; Wyatt, D. L.; Crumrine, D. S.; Cukierman, S. *Biophysical Journal* **2007**, *93*, 1571-1579.

(35) Bigaussian.

www.originlab.com/www/helponline/origin/en/UserGuide/Bigaussian.html

(accessed 8/27/2012)

APPENDIX

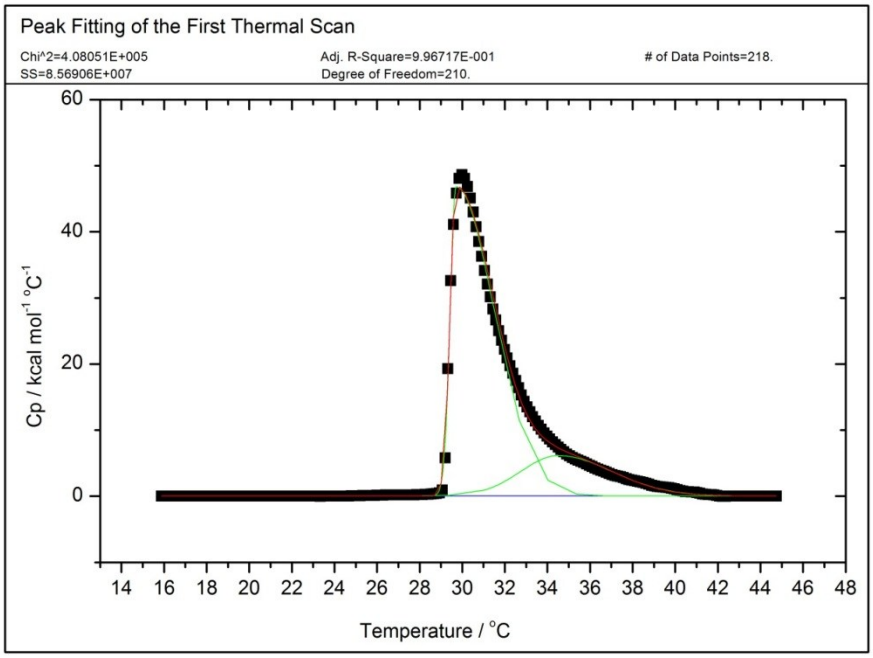
Peak Fitting of the First Thermal Scan
Chi^2=4.08051E+005
SS=8.56906E+007
Adj. R-Square=9.96717E-001
Degree of Freedom=210.
# of Data Points=218.
Cp / kcal mol-1 °C-1
Temperature / °C

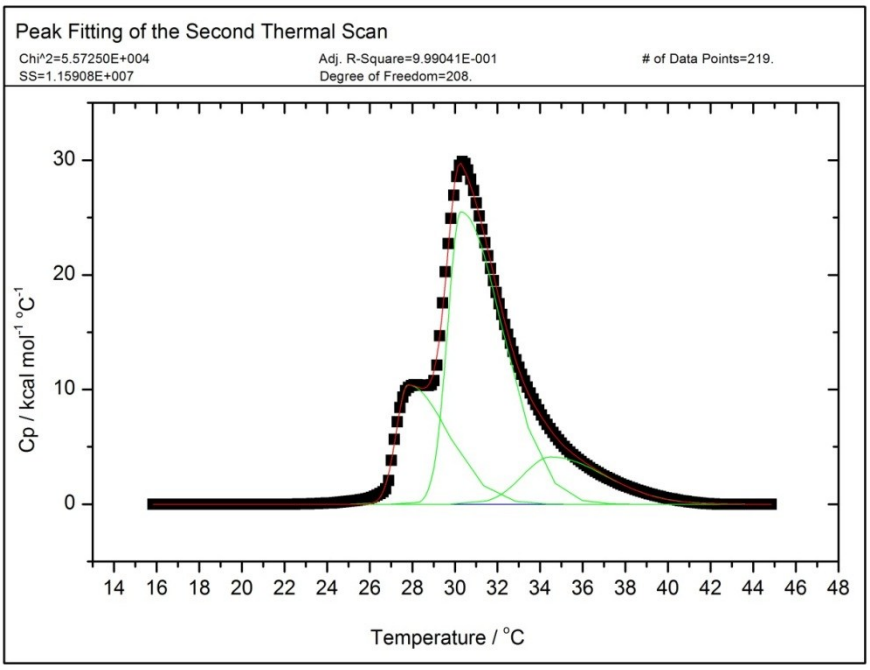
Peak Fitting of the Second Thermal Scan
Chi^2=5.57250E+004
SS=1.15908E+007
Adj. R-Square=9.99041E-001
Degree of Freedom=208.
# of Data Points=219.
Cp / kcal mol-1 °C-1
Temperature / °C

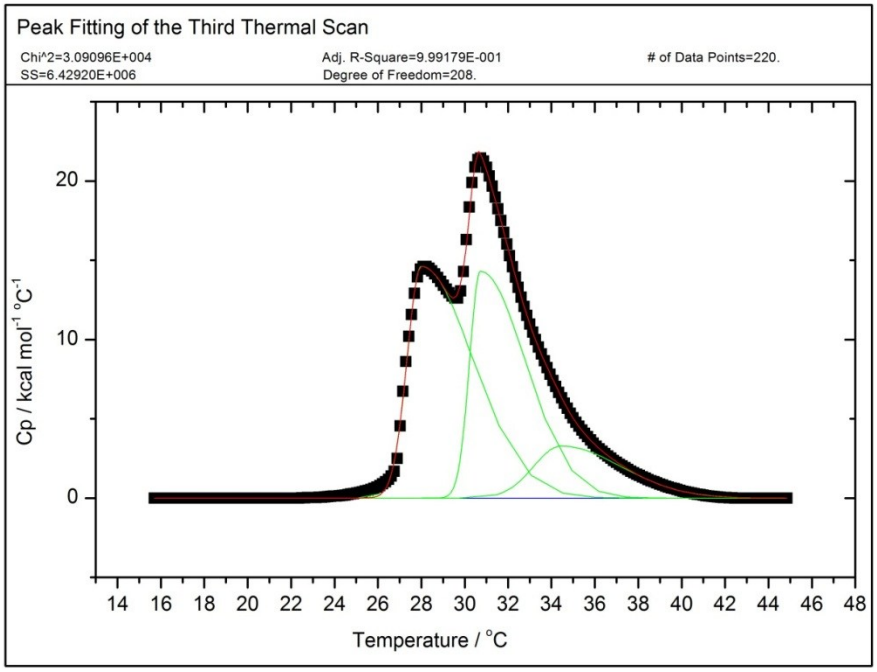
Peak Fitting of the Third Thermal Scan
Chi^2=3.09096E+004
SS=6.42920E+006
Adj. R-Square=9.99179E-001
Degree of Freedom=208.
# of Data Points=220.
Cp / kcal mol-1 °C-1
Temperature / °C

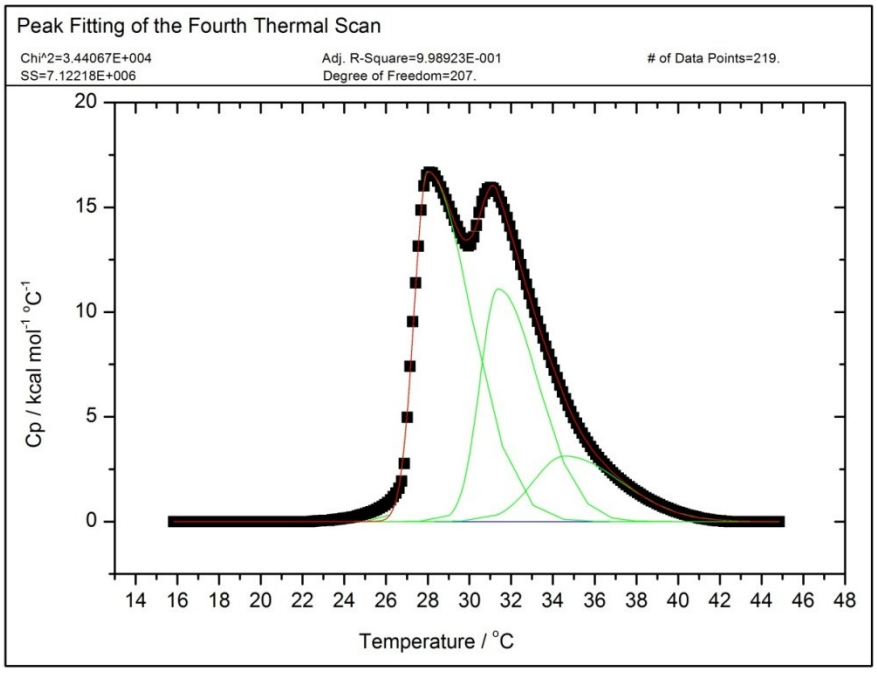
Peak Fitting of the Fourth Thermal Scan
Chi^2=3.44067E+004
SS=7.12218E+006
Adj. R-Square=9.98923E-001
Degree of Freedom=207.
# of Data Points=219.
Cp / kcal mol-1 °C-1
Temperature / °C

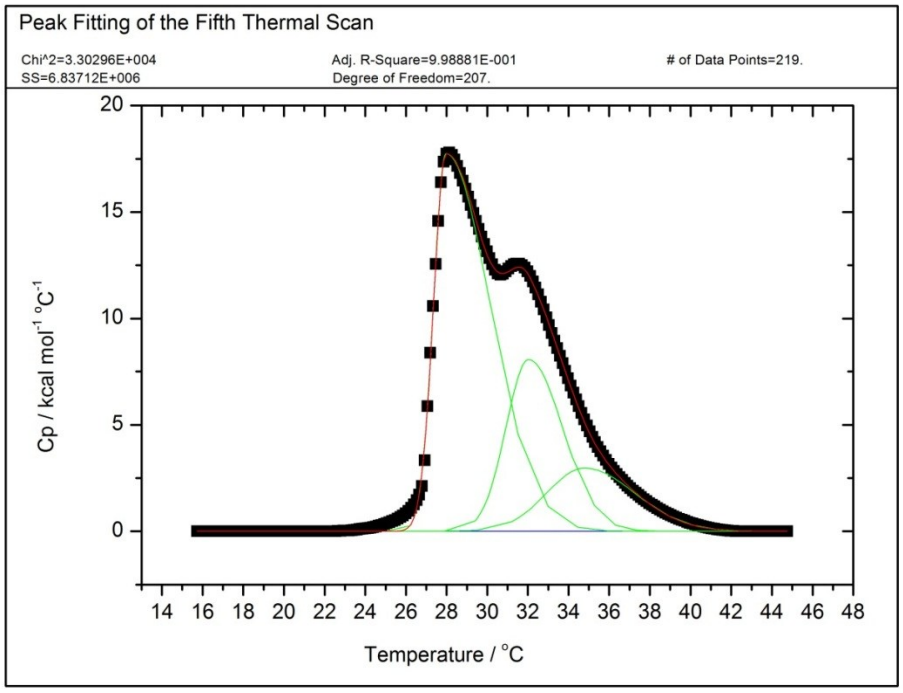
Peak Fitting of the Fifth Thermal Scan
Chi^2=3.30296E+004
SS=6.83712E+006
Adj. R-Square=9.98881E-001
Degree of Freedom=207.
# of Data Points=219.
Cp / kcal mol-1 °C-1
Temperature / °C

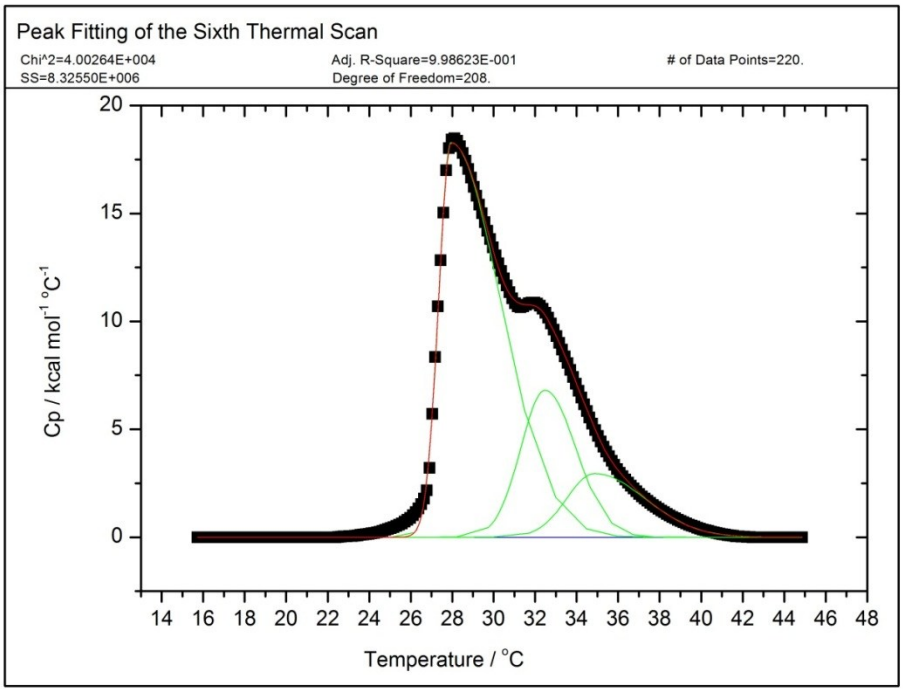
Peak Fitting of the Sixth Thermal Scan
Chi^2=4.00264E+004
SS=8.32550E+006
Adj. R-Square=9.98623E-001
Degree of Freedom=208.
# of Data Points=220.
Cp / kcal mol-1 °C-1
Temperature / °C

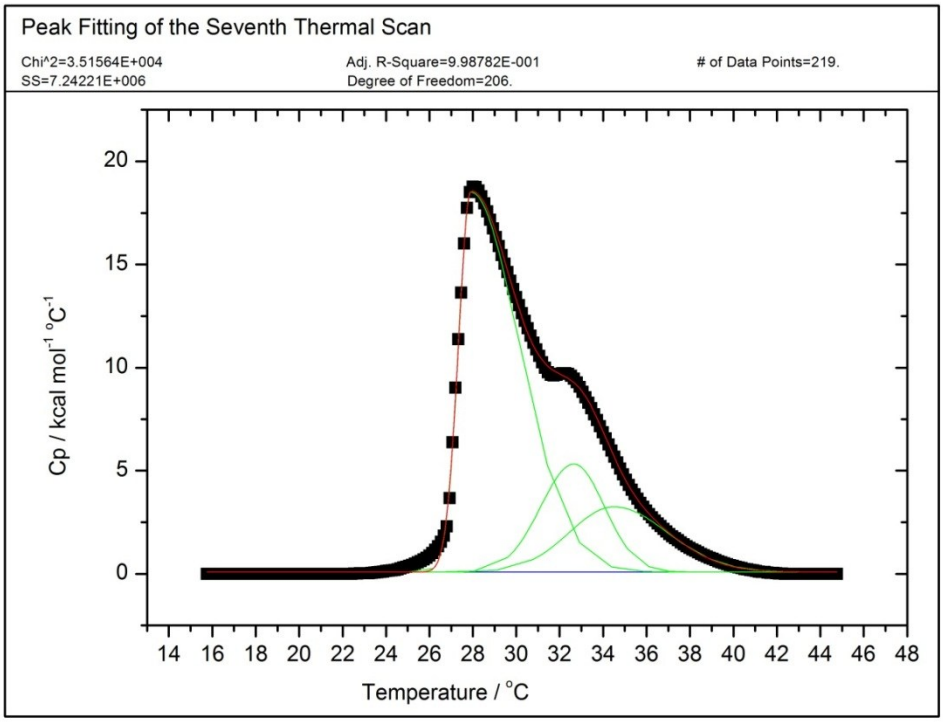
Peak Fitting of the Seventh Thermal Scan
Chi^2=3.51564E+004
SS=7.24221E+006
Adj. R-Square=9.98782E-001
Degree of Freedom=206.
# of Data Points=219.
Cp / kcal mol-1 °C-1
Temperature / °C

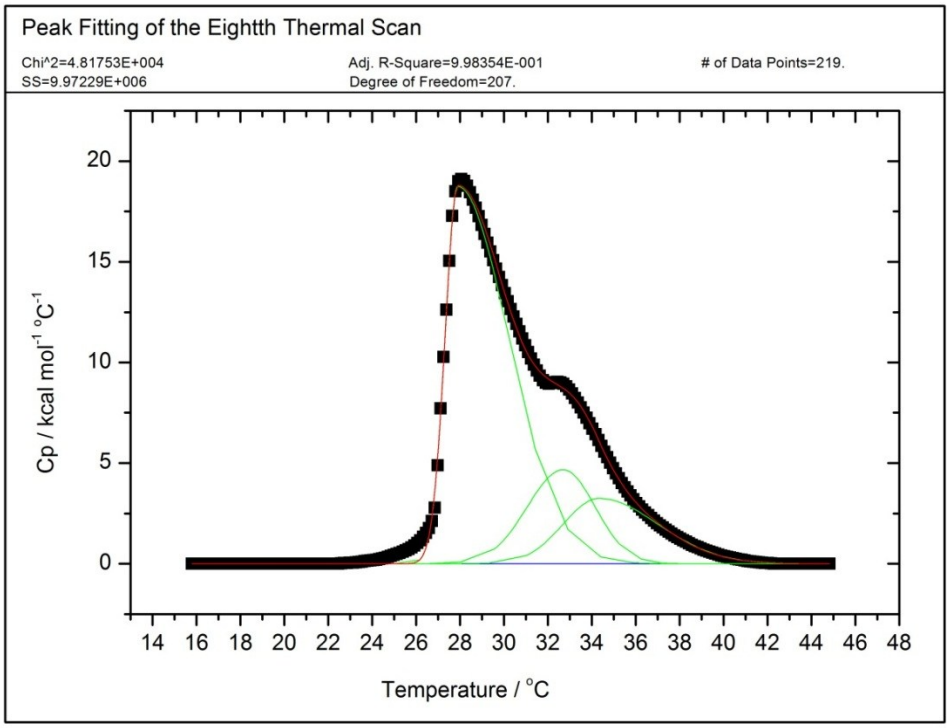
Peak Fitting of the Eightth Thermal Scan
Chi^2=4.81753E+004
SS=9.97229E+006
Adj. R-Square=9.98354E-001
Degree of Freedom=207.
# of Data Points=219.
Cp / kcal mol-1 °C-1
Temperature / °C

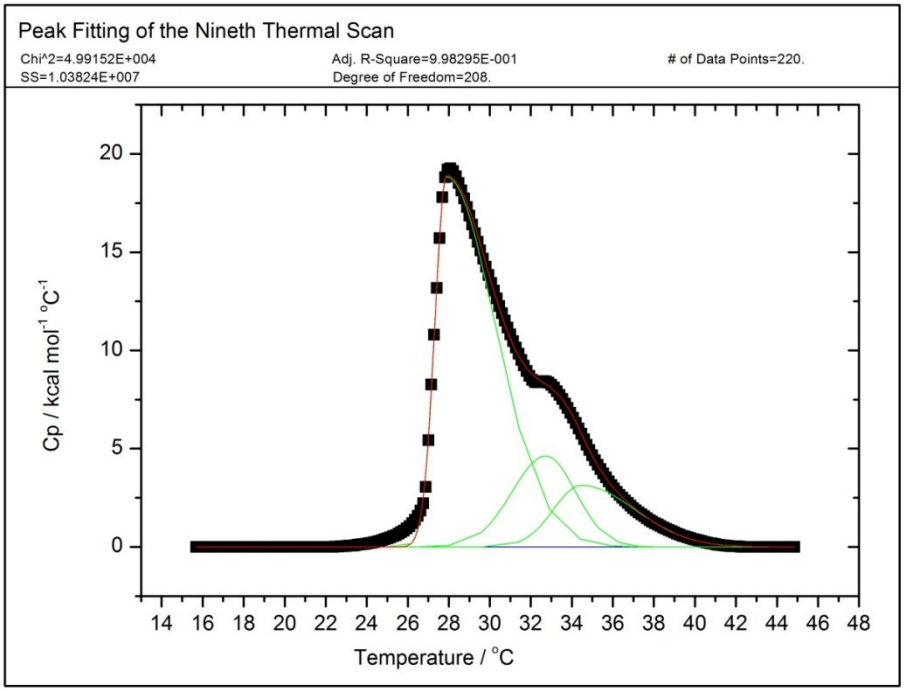
Peak Fitting of the Nineth Thermal Scan
Chi^2=4.99152E+004
SS=1.03824E+007
Adj. R-Square=9.98295E-001
Degree of Freedom=208.
# of Data Points=220.
Cp / kcal mol-1 °C-1
Temperature / °C

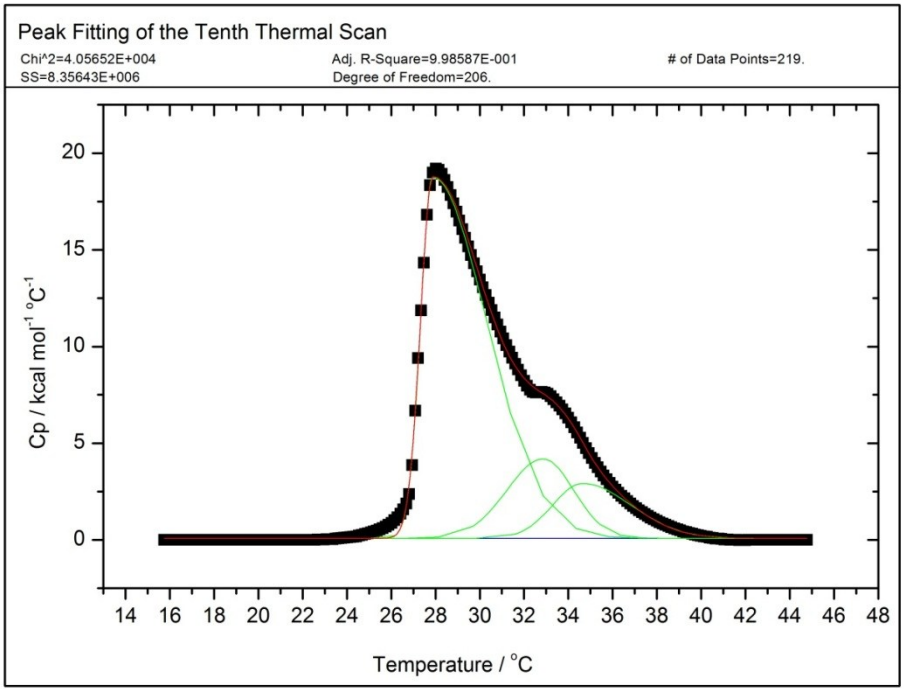
Peak Fitting of the Tenth Thermal Scan
Chi^2=4.05652E+004
SS=8.35643E+006
Adj. R-Square=9.98587E-001
Degree of Freedom=206.
# of Data Points=219.
Cp / kcal mol-1 °C-1
Temperature / °C